Nuclear Engineering and Technology 49 (2017) 1689–1695

Contents lists available at ScienceDirect

Nuclear Engineering and Technology

journal homepage: www.elsevier.com/locate/net

Original Article

Effects of temperature and solution composition on evaporation of iodine as a part of estimating volatility of iodine under gamma irradiation

Jei-Won Yeon*, Sang-Hyuk Jung

Nuclear Chemistry Research Division, Korea Atomic Energy Research Institute, 989-111 Daedeok daero, Yuseong-gu, Daejeon, 34057, Republic of Korea

ARTICLE INFO

Article history:
Received 13 November 2016
Received in revised form
26 June 2017
Accepted 21 July 2017
Available online 12 August 2017

Keywords:
Evaporation of iodine
Evaporation rate
Temperature

ABSTRACT

As a part of evaluating the volatility of iodide ions subjected to gamma irradiation, I_2 evaporation experiments were performed with I_2 and I^- mixed solutions in the temperature range 26–80°C in an open, well-ventilated space. The evaporation of I_2 was observed to follow primarily first order kinetics, depending on the I_2 concentration. The evaporation rate constant increased rapidly with increase in temperature. The presence of I^- slightly reduced the evaporation rate of I_2 by forming relatively stable I_3^-. The effect of Cl^- at <1.0 wt% on I_2 evaporation was insignificant. The evaporation rate constants of I_2 were 1.3×10^{-3} min^{-1} cm^{-2}, 2.4×10^{-2} min^{-1} cm^{-2}, and 8.6×10^{-2} min^{-1} cm^{-2}, at 26°C, 50°C, and 80°C, respectively.

1. Introduction

The volatility of radioactive iodine has been mainly of interest in the study of severe accidents at nuclear power plants, because radioactive iodine is a major radionuclide to determine the total air radioactivity around the accident area during the first number of weeks [1–3]. Therefore, many studies [4–23] have been carried out in order to understand the behavior of radioactive iodine and to minimize the impact of severe accidents. In reactor containment buildings during accidents, the radioactive iodine becomes dissolved in the cooling water directly from irradiated fuels or indirectly by the emergency spray. Iodide, which is one of the major iodine species dissolved in cooling water, is easily diffused into the gas phase after being oxidized to gaseous I_2 by gamma irradiation [4–6,11]. Next, I_2 can be converted to more volatile organic iodides, such as CH_3I, after reacting with various organic materials such as paints under high gamma irradiation [12–16]. Overall, the behavior of I_2 which is main precursor of organic iodide, is an important component used to evaluate and predict the radioactivity at an early stage of severe accidents.

To date, most iodine volatility tests were carried out with iodide solution under a high dose rate (~ k Gy/h) of gamma rays [4–6,11]. The evaporated I_2 from the I^- solution was directly measured by radiation counting or chemical analysis. This type of direct method generally provides highly reliable data about the volatilization of iodine under gamma irradiation, because the test condition was very similar to that of a real accident.

By contrast, as shown in Fig. 1, the volatilization of iodine can be divided into two connected steps. The first step (1) is the oxidation reaction of I^- to I_2 by oxidizing species such as HO·generated from water radiolysis [22,23]. The second step (2) is the evaporation of dissolved I_2 to gaseous I_2. When we predict the volatilization of iodine under various environmental conditions, it is advantageous to evaluate separately the effects of environmental factors on each step. For example, temperature is one of the main factors that affects these two steps. With increasing temperature, the rate of I^- gamma oxidation (1) decreases, while the rate of the I_2 evaporation (2) increases. Therefore, by separating the effect of temperature on these steps, we can evaluate the volatility of iodide at various temperatures more accurately. For the first step (1), which is gamma oxidation reaction of I^- to I_2(aq), considerable experimental data have been obtained on various factors, such as gamma dose, iodide concentration, and solution pH [4–6,22,23]. For the second step (2) which is evaporation of I_2(aq), various experiments and tests were carried out based on the two-film model and its extended ones [16,24]. However, relatively few experimental data have been reported [25] to date.

In the current work, we investigated the effects of temperature, concentration of I_2, and presence of I^- and Cl^- on the evaporation of

* Corresponding author.
E-mail address: yeonysy@kaeri.re.kr (J.-W. Yeon).

http://dx.doi.org/10.1016/j.net.2017.07.018

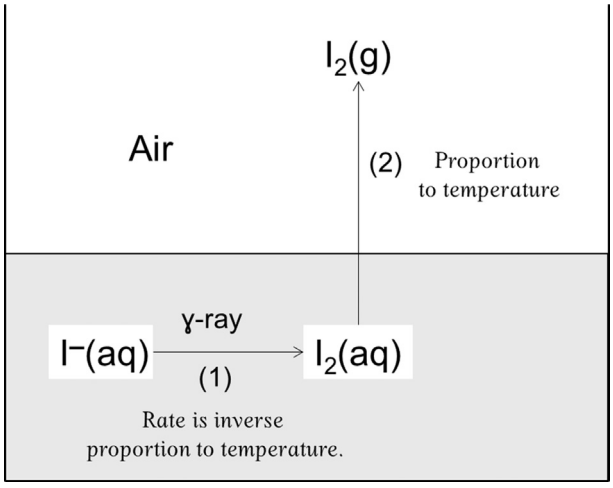

Fig. 1. Paths of iodine from I^- ion dissolved in solution to $I_2(g)$ in the air.

I_2 in I_2 and I^- mixed solutions in an open and well-ventilated space. From the experiments, we confirmed that the evaporation rate of I_2 increased exponentially as the solution temperature increased, showing a similar trend with temperature dependence of the saturated vapor pressure of I_2. We obtained the evaporation rate constant of I_2 under the temperatures of 26°C, 50°C, and 80°C. The presence of I^- was observed to slightly decrease the evaporation rate, but there was no prominent effect of Cl^- below 1.0 wt% NaCl on the evaporation of I_2. Our results will contribute to the understanding of the I_2 evaporation reaction under various environmental conditions.

2. Materials and methods

We prepared various I_2 and NaI mixed solutions for I_2 evaporation experiments. The chemical reagents used for the experiments were NaI (99.5 wt%, Sigma Aldrich, USA), I_2 (99.8 wt%, Sigma Aldrich, USA), and NaCl (99 wt%, Sigma Aldrich, USA). The I^- ion from NaI is a major chemical form of iodine released from the irradiated fuels and one of the chemical additives used in filtered containment venting system pool scrubbing. The NaCl was used for the consideration of seawater injection. However, the concentration range of each species was not determined by the consideration of any accident conditions, but rather by the detection limits of the measurement techniques we used.

The pH values of all evaporation solutions were in the range 6.1–6.5. This pH range was determined since it is the highest pH range in which I_2 is relatively stable. Above this pH range, the hydrolysis effect of I_2 cannot be ignorable in the concentration we used (~1mM), and H_2O_2 (a radiolysis products of water) starts to reduce I_2 to non-volatile I^- [22,23]. The portion of I_2 hydrolysis is less than 5% (at I_2~1mM) at pH 6.5 [26]. The pH values of all evaporation solutions were measured by a pH meter (Metrohm 654, Metrohm AG, Switzerland) at room temperature before the evaporation experiments. The solution pH definitely depends on the solution temperature, since most equilibrium reactions, even the dissociation of water molecules, depend on the temperature. In addition, the electrochemical reactions including the chemical activity of Cl^- ion working in the pH meter depend on the temperature [27]. However, in this experiment, we did not compensate the temperature effects on the solution pH and chemical reactions.

We used typical 20 mL glass vials as evaporation vessels. During the evaporation experiment, the temperature and relative humidity in the fume hood were in the range of 23 ± 2°C and 75 ± 7% relative humidity, respectively. The temperature of evaporation vessels was controlled in the range 26–80°C by a water bath. The airflow rate measured by the air velocity meter (TSI Velocicalc 8346, TSI Inc., Shoreview (MN), USA) at six points of evaporation vessels was in the range 0.81 ± 0.15 m/s. This flow rate was the maximum airflow of the fume hood, and was not determined from consideration of any reactor building condition. All I_2 evaporation experiments were carried out in the same fume hood. The schematic diagram of the evaporation experimental equipment is shown in Fig. 2.

The mixed solution of 15 mL was contained in the evaporation vessel. The height of the solution was approximately 3.5 cm from the bottom of the vessel, and the exposed area of solution for I_2 evaporation was 4.16 cm^2. In some cases, the exposed area of evaporation solution may affect I_2 evaporation. However, in this work we did not consider the effect of the exposed area on I_2 evaporation. Four or more evaporation vessels were used for a series of experiments at the same temperature. As the evaporation time passed, vessels were collected from the water bath one by one in order to measure the concentration of I_2 remaining in the solution. The I_2 concentration was measured at the ambient temperature using an ultraviolet and visible light spectrophotometer (Biochrom model WPA Lightwave II, Biochrom Ltd., Cambridge, UK) [28].

When an I_2 evaporation experiment was carried out, we placed an additional vessel containing 95.6 wt% of ethyl alcohol in the fume hood at 25 ± 1°C, outside of the water bath and measured the amounts of ethyl alcohol evaporated during each experiment. This was done to compare ventilation conditions in the fume hood. The evaporated amounts of ethyl alcohol were observed to be in the range of 0.81 ± 0.09 g/h at 23 ± 2°C and did not exhibit any dependence. This indicated that the ventilation conditions in the fume hood were almost constant during all evaporation experiments (within a range of 10%). The ethyl alcohol vessels were placed in parallel with the iodine evaporation vessels and airflow direction in order to minimize contamination by the evaporated ethyl alcohol.

3. Results and discussion

3.1. Effects of temperature and concentration on I_2 evaporation

The I_2 evaporation experiments were carried out with four different concentrations (0.05mM, 0.09mM, 0.50mM, and

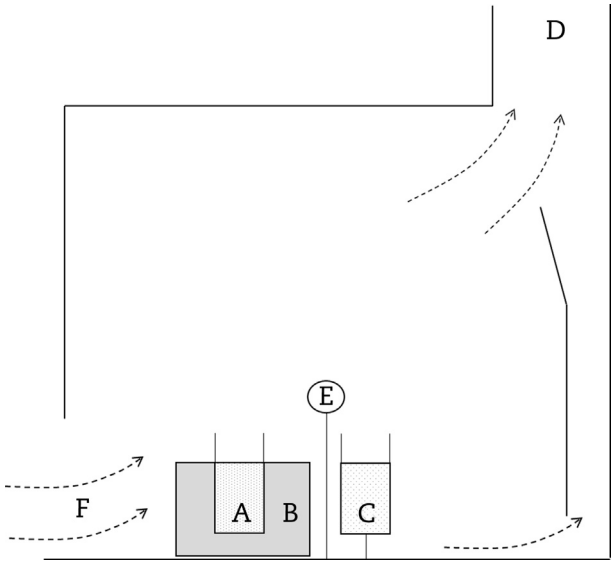

Fig. 2. The schematic diagram of the evaporation experimental equipment. (A) Iodine solution. (B) Water bath. (C) Ethyl alcohol (95.6 wt%). (D) Exhaust plenum. (E) Thermometer and humidity meter. (F) Air flow.

0.99mM) of I_2 in 5.0mM NaI solutions at 26°C, 50°C, and 80°C, respectively. Fig. 3 shows the remaining I_2 concentrations of the I_2 and NaI mixed solutions at each evaporation temperature. For all temperatures and I_2 concentrations, the concentration of I_2 in the solutions decreased exponentially as the evaporation time increased. As the temperature increased, the concentration of I_2 in the solution also decreased very rapidly. In cases where the initial I_2 concentration was 0.99mM, the lapsed times required to reduce less than 10% of the initial concentration were observed to be approximately 700 minutes at 26°C, 30 minutes at 50°C, and 7 minutes at 80°C. The results indicate that the evaporation rate of I_2 was greatly influenced by the temperature, but the initial concentration of I_2 did not have a marked effect on the evaporation rate.

At constant temperature, the evaporation reaction (2) of I_2 dissolved in solution can be expressed by a first order differential Eq. (3), which depends only on the $I_2(aq)$ concentration. With this differential equation, the evaporation rate can be expressed by Eqs. (4) and (5):

$$-d[I_2(aq)]/dt = k_{evap} \cdot A \cdot [I_2(aq)] \quad (3)$$

$$\ln\left\{I_2(aq)_{r,t} \Big/ I_2(aq)_o\right\} = -k_{evap} \cdot A \cdot t \quad (4)$$

$$\ln\left\{I_2(aq)_{r,t} \Big/ I_2(aq)_o\right\} \cdot 1/A = -k_{evap} t \quad (5)$$

where $I_2(aq)$ is the amount of I_2 dissolved in the solution, $I_2(aq)_o$ is the initial amount of I_2 dissolved in the solution, $I_2(aq)_{r,\,t}$ is the amount of remaining I_2 in the solution at evaporation time t, A is the area of solution exposed to open air space, t is the evaporation time, and k_{evap} is the evaporation rate constant of I_2.

With the relationship in Eq. (5), the data of Fig. 3 were converted and shown in Fig. 4. Because the slope of the line in Fig. 4 is $-k_{evap}$, the evaporation rate constant k_{evap} can be calculated by the linear regression of the converted evaporation data. The rate constant of evaporation increased with increase in temperature. Conversely, at constant temperature, it was observed that the evaporation rate constant was slightly influenced by the initial I_2 concentration. Thus, as the initial concentration of I_2 increased, the rate constant value decreased. The slope change caused by the initial I_2 concentration was more distinguishable at low temperature (26°C). However, the concentration effect decreased above 50°C.

The phenomenon that I_2 evaporation was expedited at higher temperature can be explained by temperature dependency of the evaporation enthalpy and saturated vapor pressure. In a closed system at constant temperature, the free energy of I_2 dissolved in water is the same as the free energy of the evaporated I_2 in the gaseous phase, when the system is in equilibrium [Eq. (6)]. At

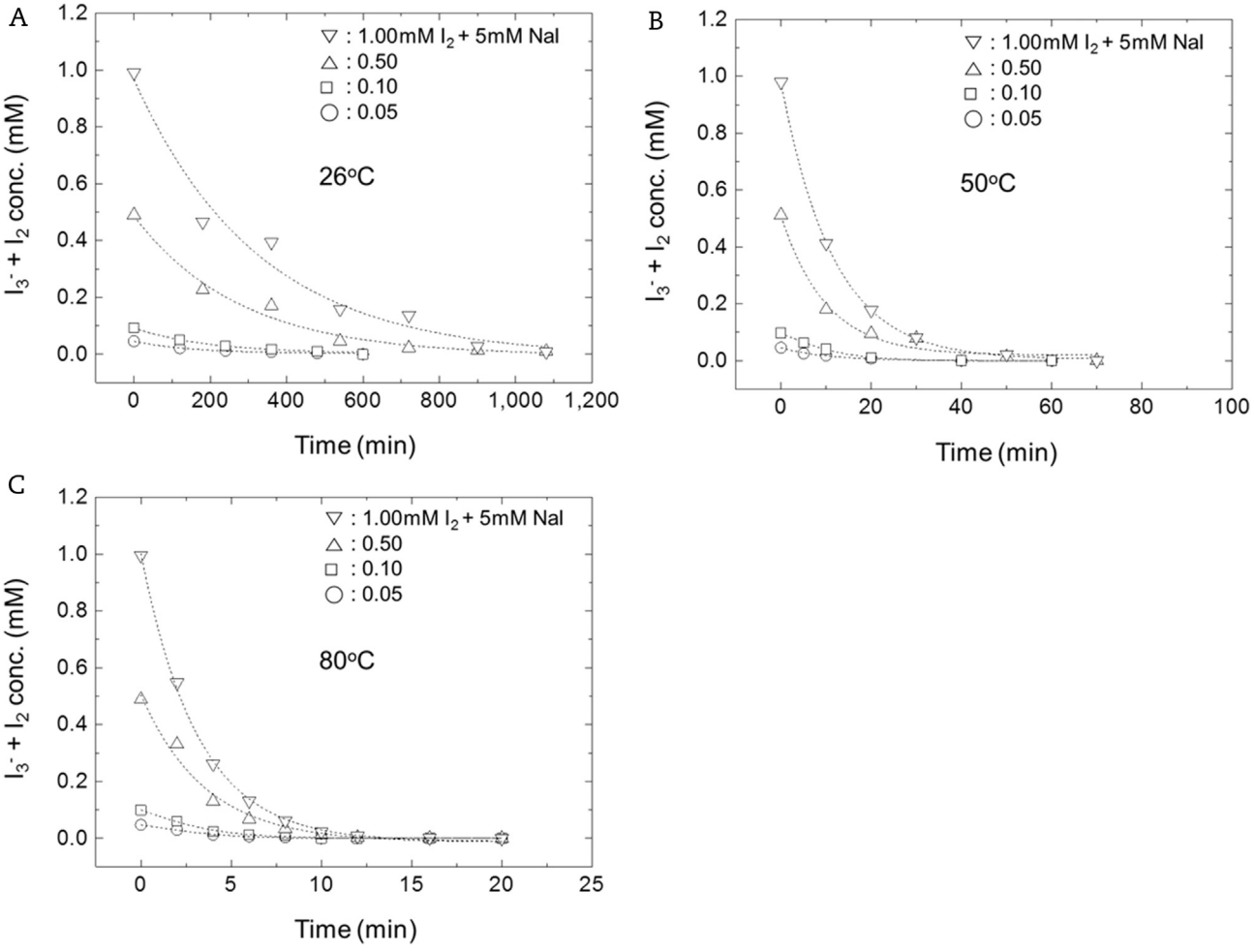

Fig. 3. Decrease of I_2 ($+ I_3^-$) concentration remaining in evaporation vessels at three different temperatures.

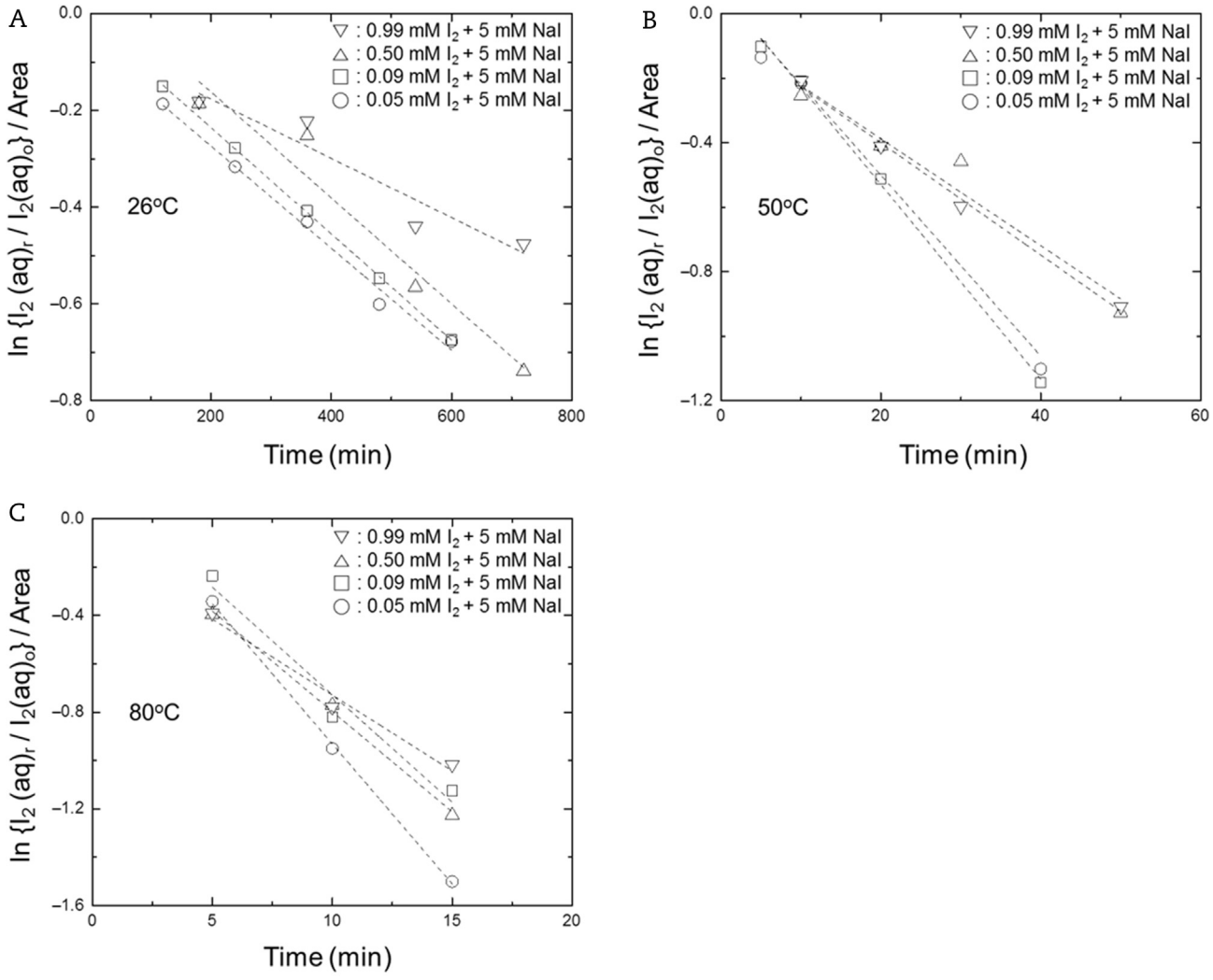

Fig. 4. Relationship between logarithmic value of iodine evaporation rate constant and evaporation time at three different temperatures. The exposed area of solution for I_2 evaporation was 4.16 cm^2.

equilibrium, therefore, the free energy change expressed by Eq. (7) should be zero.

$$I_2(\text{soluble in water}) \rightleftarrows I_2(\text{gas}) \tag{6}$$

$$\begin{aligned}\Delta G_{evap}(T) &= \Delta H_{evap}(T) - T\Delta S_{evap} \\ &= 0(\text{at equilibrium in a closed system})\end{aligned} \tag{7}$$

If the temperature of the system increases, the evaporation enthalpy ($\triangle H_{evap}$) of which the value is definitely positive decreases, because it is the latent heat required for the evaporation. In addition, the evaporation is a phase change reaction from liquid to gas, so the entropy change ($\triangle S_{evap}$) should be positive and a large value. Therefore, by increasing the temperature, both values of enthalpy ($\triangle H_{evap}$) and the entropy term ($-T\triangle S_{evap}$) in Eq. (7) decrease. Thus, the value of free energy change ($\triangle G_{evap}$) will be negative. In summary, as the temperature increases, the equilibrium [Eq. (6)] is shifted to the right and accordingly the saturated vapor pressure of I_2 increases. However, in our experiments, an equilibrium condition was never achieved, due to the well-ventilated open system. Consequently, as the temperature increased, the I_2 evaporation rate increased due to increase of the vapor pressure of I_2.

In Fig. 4, it is shown that the evaporation rate constant of I_2 decreased slightly even at constant temperature, as the initial concentration of I_2 increased. Under our experimental conditions, the concentration of I_2 is considered to play two opposing roles in its evaporation. The first role is to affect the I_2 vapor pressure in the air close to the solution surface. As the initial concentration of I_2 increases, a relatively large amount of I_2 is evaporated from the solution. Even in a well-ventilated space, the partial vapor pressure of I_2 in the air near the solution surface would be affected by the evaporated I_2. Also, this effect could reduce the evaporation rate of I_2 when the initial concentration is high. The second role is to affect the stability of I_2 in mixed I_2 and NaI solutions. In the presence of I^-, as shown in Eq. (8), I_2 dissolved in the solution reacts rapidly with I^- and forms a relatively stable species I_3^-. Under our experimental conditions, the I^- concentration of the mixed solutions was constant at 5.0mM. At constant I^- concentration, as the I_2 concentration increased, the partial ratio of stable I_3^- decreased and the condition was more favorable to evaporation of I_2 [29]:

$$I_2(aq) + I^- \rightleftarrows I_3^- \quad K_{eq} = 695\ (\text{at } 298K), 421\ (\text{at } 323K) \tag{8}$$

In our experiments, as the concentration of I_2 increased, the evaporation rate constant of I_2 decreased slightly at constant

temperature. This result clearly indicates that the influence of I_2 related to the formation of stable I_3^- would be overwhelmed by another influence of I_2 on the vapor pressure of I_2 in the air close to the solution surface.

3.2. Relationship between evaporation rate constant and saturated vapor pressure of I_2

In Section 3.1, we confirmed that the evaporation rate was slightly influenced by the initial concentration of I_2, especially at high concentration. Therefore, in order to minimize the concentration dependency, we chose the evaporation rate constant measured with the lowest concentration of I_2. Next, we evaluated the effect of temperature on the evaporation rate constant. In Fig. 5, the evaporation rate constants obtained from 0.05mM I_2 solutions were plotted against the evaporation temperature. The evaporation rate constant exponentially increased with increase in the temperature. By curve fitting of Fig. 5, we developed an empirical formula [Eq. (9)] for the relationship between I_2 evaporation rate constant and temperature, and denoted it as a dotted line:

$$k_{evap}(T) = 0.00795 \cdot \exp(0.0354\,T) - 0.01888 \quad (9)$$

where $k_{evap}(T)$ is the I_2 evaporation rate constant at temperature T and T is temperature (°C).

As mentioned in Section 3.1, the vapor pressure of I_2 at the evaporation temperature is one of the major driving forces to evaporate I_2 to the open environment. In Fig. 5, the evaporation rate constant was compared to the saturated vapor pressure [30] of I_2 according to the temperature. It is shown that both trends were very similar as the temperature increased. Generally, the gas-liquid transfer processes (like evaporation) can be demonstrated by assuming a two-film model [16,24], and highly soluble gases are known to have transfer rates controlled by gas-phase films [31]. Under our experimental conditions, the saturated vapor pressure of I_2 definitely affects the I_2 concentration in the gas-phase film of the two-film model. Therefore, the similar trends of the evaporation rate constant and the saturated vapor pressure of I_2 indicate that the gas-phase film is the rate limiting layer in the I_2 evaporation reaction.

By contrast, we also applied an Arrhenius plot to the relationship using the I_2 evaporation rate constant and temperature. From the plot analysis, we obtained a poor linearity between the logarithmic value of the evaporation rate constant and the inverse absolute temperature. This finding means that there are two or more factors (or processes) dependent on temperature involved in the I_2 evaporation reaction, and that the evaporation reaction is not controlled by just one of them. In fact, evaporation is generally regarded as a multiprocess reaction [32]. For I_2 continuously evaporating from solution, I_2 in water must transport to the water surface layer contacted with air, latent heat had to be supplied to I_2 to overcome the stabilized energy gap of I_2 between water and gas phases, and the evaporated I_2 gas should be moved into the air away from the solution surface. Therefore, the evaporation rate depends on many factors such as the mobility of I_2 in water, the attractive power between I_2 and H_2O molecules, and the partial vapor pressures of evaporated gases, such as I_2 and H_2O. Also, most of these factors closely depend on the temperature. In summary, because each process in the I_2 evaporation reaction depends on the temperature, it is difficult to understand the temperature dependency of the evaporation rate constant with only an Arrhenius relationship.

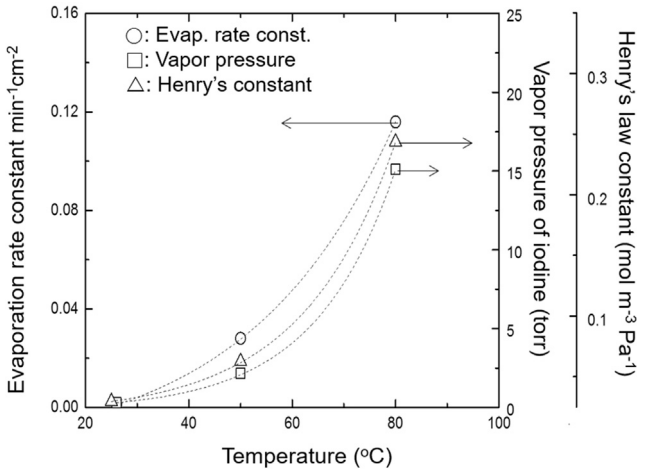

Fig. 5. Relationship between the evaporation rate constant and the saturated vapor pressure of I_2 according to the evaporation temperature.

3.3. Effects of I^- and Cl^- on the evaporation rate constant of I_2

In Section 3.1, we mentioned that the presence of I^- might retard the evaporation of I_2 in forming a relatively stable I_3^- species in the solution. In order to investigate the effect of I^- quantitatively, we carried out I_2 evaporation experiments at 80°C using 0.88 ± 0.02mM I_2 solutions with four different NaI concentrations (0mM, 1.0mM, 5.0mM, and 25mM).

Fig. 6A shows the changes in concentration of the remaining I_2 (or I_3^-) in the mixed solutions according to the evaporation time. Until the NaI concentration was 1.0mM, which is almost the same concentration as I_2, little effect of NaI was observed on the I_2 evaporation. However, above 5.0mM NaI, the I_2 evaporation reaction was gradually retarded. This can be explained because more I_3^- could be formed as the concentration of NaI increased. Thus, the equilibrium reaction [Eq. (6)] was shifted to the right by the addition of NaI. In Fig. 6B, the concentration data of Fig. 6A was converted and plotted in the format of an evaporation rate Eq. (5). The results of all four different NaI concentrations show a very clear linear relationship. The values of evaporation rate constants obtained from the slopes of the lines decreased (0.117 min^{-1} cm^{-2}, 0.114 min^{-1} cm^{-2}, 0.086 min^{-1} cm^{-2}, and 0.046 min^{-1} cm^{-2}) as the NaI concentration increased (0mM, 1mM, 5mM, up to 25mM, respectively).

The result indicates that I^- mitigates the evaporation of I_2 at 80°C, because the fraction of I_3^-, which is the more stable species, increases with increase in the I^- concentration, according to the equilibrium reaction [Eq. (8)]. We plotted the relationship between the rate constant of I_2 evaporation and I^-/I_2 in Fig. 7. It was observed that the evaporation rate constant decreased exponentially as the concentration ratio of I^- to I_2 (I^-/I_2) increased. By curve fitting of the data in Fig. 7, we developed an empirical formula [Eq. (10)] between the evaporation rate constant of I_2 and the ratio I^-/I_2. From the formula, we found that the evaporation rate constant of I_2 at 80°C approached the minimum value (0.0402), as the molar concentration ratio of I^- to I^-_2 increased. This means that the I_3^- concentration was not affected significantly when the ratio of I^- to I^-_2 increased more than 30. This formula [Eq. (10)] could be useful to evaluate the evaporation rate of I_2 in the presence of I^- like pool scrubbing of filtered containment venting system. However, our experimental condition was not determined from consideration on a certain accident condition:

$$k_{80}(R) = 0.0788 \cdot \exp(-0.0921\,R) + 0.0402 \quad (10)$$

where $k_{80}(R)$ is the evaporation rate constant of I_2 at 80°C and R is the molar concentration ratio of I^- to I_2^-.

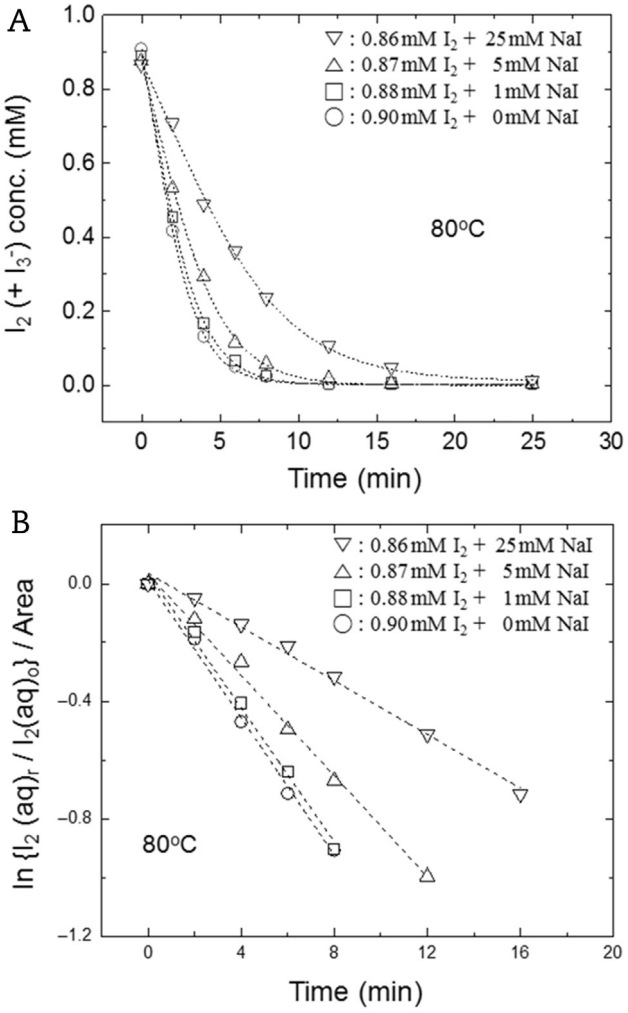

Fig. 6. Effect of iodide concentration on the evaporation of iodine. I_2 concentration: 0.88 ± 0.02mM, I^- concentration: 0mM, 1.0mM, 5.0mM, 25mM. Evaporation temperature: 80°C.

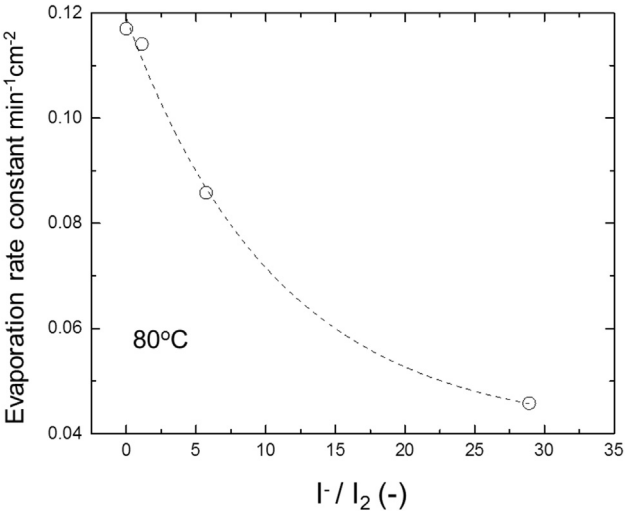

Fig. 7. Relationship between the rate constant of I_2 evaporation and I^-/I_2 in the temperature range 26–80°C.

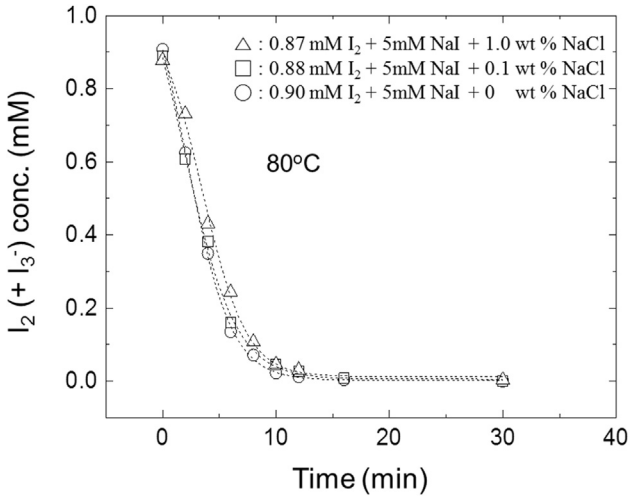

Fig. 8. Effect of Cl^- on the evaporation of I_2. I_2 concentration: 0.88 ± 0.02mM, NaI concentration: 5.0mM, NaCl concentration: 0wt%, 0.1wt%, 1.0 wt%. Evaporation temperature: 80°C.

Because sea water could be considered for an emergency cooling water of a nuclear reactor in an accident case, the effect of Cl^- was also investigated on the I_2 evaporation. The evaporation experiments were carried out with I_2 and NaCl mixed solutions at 80°C. We also measured the remaining I_2 concentrations in the solutions and plotted the values in Fig. 8. Although very weak retardation of I_2 evaporation was observed up to 1.0 wt% NaCl, there was no substantial effect on the I_2 evaporation. This result means that there is little effect of Cl^- on the I_2 evaporation step, even if about 30% of cooling water is replaced by seawater. Upon considering that 1.0 wt % NaCl is converted to 0.17M NaCl, we easily found that the effect of Cl^- on the I_2 evaporation was very weak compared to that of I^- as shown in Fig. 6B.

For the I_2 and Cl^- mixed solution, no electrochemical reduction and oxidation reactions are considered because the oxidation power of I_2 is considerably stronger than that of Cl_2. However, it is known that the solubility (0.029 g in 100 g water at 20°C) of I_2 is greatly enhanced by the addition of NaCl [33]. This phenomenon means that I_2 molecules in the aqueous solution are probably stabilized by the presence of Cl^-. However, this stabilization by Cl^- was not sufficiently strong to retard I_2 evaporation in the NaCl concentration range < 1.0 wt%. It should be noted that we investigated the effect of Cl^- on the evaporation of I_2 [denoted as Step (2) in Fig. 1], not on the overall volatilization process of iodine under gamma irradiation. However, in Step (1) under gamma irradiation, there are complex chemical reactions in the I_2, I^-, and Cl^- mixed system, which are not mentioned in this work. Therefore, this result is only valid for the evaporation process of I_2.

4. Conclusion

The evaporation reaction of I_2 was confirmed to follow primarily first order reaction kinetics depending on the concentration of I_2 dissolved in the solution. As the temperature increased (26°C, 50°C, and 80°C), the evaporation rate constant of I_2 increased rapidly (1.3×10^{-3} min^{-1} cm^{-2}, 2.4×10^{-2} min^{-1} cm^{-2}, and 8.6×10^{-2} min^{-1} cm^{-2}, respectively). However, as the ratio of I^- to I_2 increased in the range 0–28 at the constant I_2 concentration of 0.88mM, the evaporation rate constant of I_2 decreased gradually. From the similar temperature dependences of the evaporation rate constant

and the saturated vapor pressure of I_2, the gas-phase film was demonstrated as the rate limiting layer in I_2 evaporation reaction. We developed two empirical formulas regarding the effects of temperature and I^- concentration on the I_2 evaporation rate constant. The retardation of I_2 evaporation in the presence of I^- was attributed to the formation of stable I_3^-. Conversely, the interference of Cl^- in I_2 evaporation was so weak that it was difficult to observe in the concentration range <1.0 wt% NaCl. In this work, we focused only on the evaporation of dissolved I_2 to gaseous I_2. Therefore, this result is only valid for the evaporation process of I_2, not for the overall volatilization of iodine under gamma irradiation.

Conflicts of interest

All authors have no conflicts of interest to declare.

Acknowledgments

This work was supported by National Research Foundation of Korea (NRF) grants (2017M2A8A4015281, 2017M2A8A5014710), funded by the Korean government (MSIT).

References

[1] J. Ishida, N. Miyagawa, H. Watanabe, T. Asano, Y. Kitahara, Environmental radioactivity around Tokai-works after reactor accident at Chernobyl, J. Environ. Radioact. 7 (1988) 17–27.
[2] K. Hirose, 2011 Fukushima Dai-ichi nuclear power plant accident: summary of regional radioactivity deposition monitoring results, J. Environ. Radioact. 111 (2012) 13–17.
[3] N. Momoshima, S. Sugihara, R. Ichikawa, H. Yokoyama, Atmospheric radionuclides transported to Fukuoka, Japan remote from the Fukushima Dai-ichi nuclear power complex following the nuclear accident, J. Environ. Radioact. 111 (2012) 28–32.
[4] C.-C. Lin, Chemical effects of gamma radiation on iodine in aqueous solutions, J. Inorg. Nucl. Chem. 42 (1980) 1101–1107.
[5] K. Ishigure, H. Shiraishi, H. Okuda, N. Fujita, Effect of radiation on chemical forms of iodine species in relation to nuclear reactor accidents, Radiat. Phys. Chem. 28 (1986) 601–610.
[6] K. Ishigure, H. Shiraishi, H. Okuda, Radiation chemistry of aqueous iodine systems under nuclear reactor accident conditions, Radiat. Phys. Chem. 32 (1988) 593–597.
[7] J.C. Wren, J. Paquette, S. Sunder, B.L. Ford, Iodine chemistry in the +1 oxidation state. II. A Raman and UV-visible spectroscopic study of the disproportionation of hypoiodite in basic solutions, Can. J. Chem. 64 (1986) 2284–2296.
[8] M. Lucas, Radiolysis of cesium iodide solutions in conditions prevailing in a pressurized water reactor severe accident, Nucl. Technol. 82 (1988) 157–161.
[9] E.C. Beahm, C.F. Weber, T.S. Kress, G.W. Parker, Iodine Chemical Forms in LWR Severe Accidents, NUREG/CR-5732, ORNL/TM-11861, US-NRC, ORNL, Oak Ridge (TN), 1992.
[10] M.E. Berzal, M.J.M. Crespo, M.S. Kowaiczyk, M.M. Espigares, J.L. Jimenez, State-of-the-art Review on Fission Products Aerosol Pool Scrubbing under Severe Accident Conditions, EUR 16241 EN, Nuclear Science and Technology, EC, 1995.
[11] C.B. Ashmore, J.R. Gwyther, H.E. Sims, Some effects of pH on inorganic iodine volatility in containment, Nucl. Eng. Des. 166 (1996) 347–355.
[12] J.C. Wren, J.M. Ball, G.A. Glowa, The chemistry of iodine in containment, Nucl. Technol. 129 (2000) 297–325.
[13] F. Taghipour, G.J. Evans, Radiolytic organic iodide formation under nuclear reactor accident conditions, Environ. Sci. Technol. 34 (2000) 3012–3017.
[14] L. Cantrel, Radiochemistry of iodine outcomes of the caiman program, Nucl. Technol. 156 (2006) 11–28.
[15] N. Girault, S. Dickinson, F. Funke, A. Auvinen, L. Herranz, E. Krausmann, Iodine behaviour under LWR accident conditions: lessons learnt from analyses of the first two Phebus FP tests, Nucl. Eng. Des. 236 (2006) 1293–1308.
[16] B. Clément, L. Cantrel, G. Ducros, F. Funke, L. Herranz, A. Rydl, G. Weber, C. Wren, State of the Art Report on Iodine Chemistry, NEA/CSNI/R(2007)1, OECD-NEA, Paris, 2007.
[17] G.V. Buxton, Q.G. Mulazzani, On the hydrolysis of iodine in alkaline solution: a radiation chemical study, Radiat. Phys. Chem. 76 (2007) 932–940.
[18] L. Bosland, F. Funke, N. Girault, G. Langrock, PARIS project: radiolytic oxidation of molecular iodine in containment during a nuclear reactor severe accident. Part 1. Formation and destruction of air radiolysis products–Experimental results and modeling, Nucl. Eng. Des. 238 (2008) 3542–3550.
[19] L.E. Herranz, B. Clément, In-containment source term: key insights gained from a comparison between the PHEBUS-FP programme and the US-NRC NUREG-1465 revised source term, Prog. Nucl. Energy 52 (2010) 481–486.
[20] S. Dickinson, F. Andreo, T. Karkela, J. Ball, L. Bosland, L. Cantrel, F. Funke, N. Girault, J. Holm, S. Guilbert, L.E. Herranz, C. Housiadas, G. Ducros, C. Mun, J.-C. Sabroux, G. Weber, Recent advances on containment iodine chemistry, Prog. Nucl. Energy 52 (2010) 128–135.
[21] H.-C. Kim, Y.-H. Cho, Raim – a model for iodine behavior in containment under severe accident condition, Nucl. Eng. Technol. 47 (2015) 827–837.
[22] S.-H. Jung, J.-W. Yeon, S.Y. Hong, Y. Kang, K. Song, The oxidation behavior of iodide ion under gamma irradiation conditions, Nucl. Sci. Eng. 181 (2015) 191–203.
[23] S.Y. Hong, S.-H. Jung, J.-W. Yeon, Effect of aluminum metal surface on oxidation of iodide under gamma irradiation conditions, J. Radioanal. Nucl. Chem. 308 (2016) 459–468.
[24] C.F. Weber, E.C. Beahm, T.S. Kress, Models of Iodine Behavior in Reactor Containments, ORNL/TM-12202, Oak Ridge National Laboratory, Oak Ridge (TN), 1992.
[25] M.J. Polissar, The rate of evaporation of chlorine, bromine, and iodine from aqueous solutions, J. Chem. Educ. 12 (1935) 89–92.
[26] I. Lengyel, I.R. Epstein, K. Kustin, Kinetics of iodine hydrolysis, Inorg. Chem. 32 (1993) 5880–5882.
[27] D.D. Macdonald, A.C. Scott, P. Wentrcek, Silver-silver chloride thermocells and thermal liquid junction potentials for potassium chloride solutions at elevated temperatures, J. Electrochem. Soc. 126 (1979) 1618–1624.
[28] S.-H. Jung, J.-W. Yeon, Y. Kang, K. Song, Determination of triiodide ion concentration using UV-visible spectrophotometry, Asian J. Chem. 26 (2014) 4084–4086.
[29] D.A. Palmer, R.W. Ramette, R.E. Mesmer, Triiodide ion formation equilibrium and activity coefficients in aqueous solution, J. Solution Chem. 13 (1984) 673–683.
[30] G.P. Baxter, C.H. Hickey, W.C. Holmes, The vapor pressure of iodine, J. Am. Chem. Soc. 29 (1907) 127–136.
[31] S.E. Jorgensen, Studies in Environmental Science 5: Industrial Waste Water Management, Elsevier Scientific Publishing Company, Amsterdam, Netherlands, 1979.
[32] F.E. Jones, Evaporation of Water: with Emphasis on Applications and Measurements, Lewis Publishers, Chelsea (MI), USA, 1992.
[33] C.L. Harman, The Solubility of Iodine in Aqueous Salt Solutions, Master's Thesis in Chemistry, Georgia School of Technology, 1932.